

Rapid-thermal post-annealing effect of room-temperature grown ZnO : Ga layers by the radio-frequency co-sputtering

J. H. Yu^a, H. J. Yang^a, H. S. Mo^a, T. S. Kim^a, T. S. Jeong^a, C. J. Youn^{a,*} and K. J. Hong^b

^aSemiconductor Physics Research Center (SPRC), School of Semiconductor and Chemical Engineering, Chonbuk National University, Jeonju 561-756, Korea

^bDepartment of Physics, Chosun University, Gwangju 501-759, Korea

The ZnO : Ga layers were grown on the Al₂O₃ substrate by using the radio frequency (RF) magnetron co-sputtering system at room temperature (RT), varying the RF power of the Ga₂O₃ target. The RT as-grown ZnO : Ga layers were post-annealed by the rapid thermal annealing (RTA) method with various temperatures. Ga-40 of the RT as-grown ZnO : Ga layers showed an excellent crystallinity. Also, the transmittance of Ga-40 annealed at the RTA temperatures of over 300 °C was very transparent, with the transmittance exceeding 80%. Thus, the optical band-gap energy ranged from 3.4548 to 3.8118 eV according to the variation of the RTA temperature. This band-gap energy showed a tendency to increase until the RTA temperature of 400 °C, and then a decrease was observed. The lowest values of resistivity and sheet resistance were extracted from Ga-40 annealed at 400 °C; their values were $5.04 \times 10^{-4} \Omega \cdot \text{cm}$ and $21.24 \Omega/\square$, respectively. The obtained parameters were equal to those of the ZnO : Ga layer grown for maintaining the substrate temperature of 400 °C. Consequently, this result indicates that the time reduction and the simplified fabrication for device applications of the ZnO : Ga layers can be achieved through the RTA method of short-time thermal-annealing after RT growth.

Key words: ZnO : Ga, Sputter, RTA, Characterization, Room temperature growth.

Introduction

Wide band-gap zinc oxide (ZnO) is one of the important transparent conductive oxides (TCO), which are used as transparent electrodes in various fields such as solar cells and flat panel display devices, requiring the resistivity to be below $10^{-4} \Omega \cdot \text{cm}$, optical transmission above 80%, and an optical band gap larger than that of 3 eV. However, undoped ZnO itself has a high resistivity due to a low carrier concentration, in spite of having excellent optical properties. So, in order to improve electrical property, the dopant materials of Al, In, and Ga were injected in ZnO. Of these dopant materials, Al leads to a high reactivity with oxygen during the growth of the layer, through heavily doped Al with high conductive TCO layers. But, the Ga dopant is less reactive and has more resistant oxidation compared to Al. Also, the covalent bond length of Ga-O (1.92 Å) is smaller than that of Zn-O (1.97 Å), which minimizes ZnO lattice deformations, even at high Ga concentrations [1, 2]. Because of these reasons, Ga has been used as a dopant material in ZnO for TCO. The growth of the Ga-doped ZnO (ZnO : Ga) layers have been achieved

by several techniques such as radio frequency (RF) magnetron sputtering, pulsed laser deposition, metal organic chemical vapor deposition (MOCVD), and spray pyrolysis, etc [3-6]. Thus, while growing ZnO : Ga through these methods, the substrate temperature generally has a high growth temperature [7]. Thereafter, the as-grown ZnO : Ga layers were post-annealed for a long time [8, 9]. However, it suggests that these processes disturb a concise fabrication of ZnO : Ga.

In this paper, we grew the ZnO : Ga layers on the Al₂O₃ substrate by using the RF magnetron co-sputtering system at room temperature (RT). The post annealing on as-grown ZnO : Ga layers was conducted by using the rapid thermal annealing (RTA) method with various temperatures. Electro and optical properties on post-annealed ZnO : Ga layers were discussed.

Experimental Procedure

ZnO : Ga layers were grown using a commercial RF magnetron sputtering system (Aja International Inc., USA) with an automatic matching network. ZnO (5N, KURT, USA) and Ga₂O₃ (4N, LST, USA) targets, two-inches in diameter, were loaded into the sputtering chamber. In order to have a uniform layer thickness, the rotating speed of the substrate was kept at 40 rpm during the deposition. The target-substrate distance was set at 10 cm. The substrate used for the ZnO : Ga

*Corresponding author:
Tel : +82-63-270-3651
Fax: +82-63-270-3585
E-mail: cjyoun@chonbuk.ac.kr

layers was (0001) Al_2O_3 . The base pressure was evacuated to a pressure lower than 1.3×10^{-8} Torr. Prior to the ZnO : Ga layer growth, the surface of the substrate was cleaned with acetone and ethanol for 5 min and was etched in $\text{H}_2\text{SO}_4 : \text{H}_3\text{PO}_4 = 3 : 1$ for 7 min. Then, it was rinsed in deionized water. The loaded target was continuously pre-sputtered for 30 min under a 50 W RF power to remove any surface contamination of the target. In order to grow the ZnO : Ga layers, the RF power of the ZnO target was fixed to 80 W and the Ga flux was controlled by varying the RF power of the Ga_2O_3 target. The RF powers of the Ga_2O_3 target were varied from 20, 40, and 60 W. Thereafter, they were labeled as a Ga-20, -40, and -60, respectively. During the ZnO : Ga layer growth, the injected Ar gas to create ambient pressure as background flows was 50 sccm and the working pressure was set at 4 mTorr. Also, the substrate temperature during the co-sputtering growth was fixed to RT. The thickness of the layers was about 200 nm by adjusting sputtering time. Thereafter, the as-grown ZnO : Ga layers were post-annealed by using the RTA method at the temperatures of 200, 300, 400, 500, and 600 °C for 1 min in N_2 ambient. The crystal structure of deposited layers was analyzed by an X-ray diffraction (XRD) experiment. Also, the optical transmission spectra were investigated with an ultraviolet (UV) visible infrared spectrometer. In order to drag out the electric property, the four point probe measurement was conducted.

Results and Discussion

ZnO : Ga layers grown at RT by varying the RF power of Ga_2O_3 target

ZnO : Ga layers were grown by varying the RF power of the Ga_2O_3 target. During the ZnO : Ga layer growth, the substrate temperature was maintained at RT. Fig. 1 shows the rocking curves of the XRD ω - 2θ scans on the RT grown ZnO : Ga layers by varying the RF power of Ga_2O_3 target. As shown in Fig. 1, two dominant peaks appeared in the rocking curves of the XRD. These patterns correspond to the diffraction peaks of the ZnO (0002) and Al_2O_3 (0006). Also, for the Ga-40 case, the peak of low intensity observed at a high diffraction angle and its phase was the ZnO (0004). No peak of any other phase, except these peaks, was observed. This fact indicates that the layers are strongly oriented to the c-axis of hexagonal

structure and also crystallized under constraints created by the substrate. In order to evaluate the mean crystallite size of the film, it was analyzed by using the Scherrer formula [10]:

$$D = 0.94\lambda / (B \cos\theta), \quad (1)$$

where λ , θ , and B are the X-ray wavelength (0.15405 nm), the Bragg diffraction angle, and a full width at half maximum (FWHM) value on (0002) peak in radians, respectively. Also, the biaxial stress can be calculated from the formula [11]:

$$\sigma = -453 \times 10^9 (c - c_0) / c_0, \quad (2)$$

where c is the measure value of the c-axis lattice parameter and c_0 is the strain-free parameter $c_0 = 0.5206$ nm. Table 1 listed the structural parameters of ZnO : Ga obtained from the XRD experiment by varying the RF power of the Ga_2O_3 target. As compared with ZnO, the lattice constant c of Ga-20 is almost independent of the Ga content, indicating the ZnO structure. It is nearly free on the biaxial stress too. Therefore, it suggests that the Ga ions acted as the dopant, like an impurity in ZnO. As shown in the subfigure, the magnified (0002) peaks shifted into a low diffraction angle by increasing the RF power of the Ga_2O_3 target. It can be considered that the Ga ions according to the increase of the Ga contents in the layer are participated to the interstitial type in the ZnO lattices. In this case, the biaxial stress in the layer can

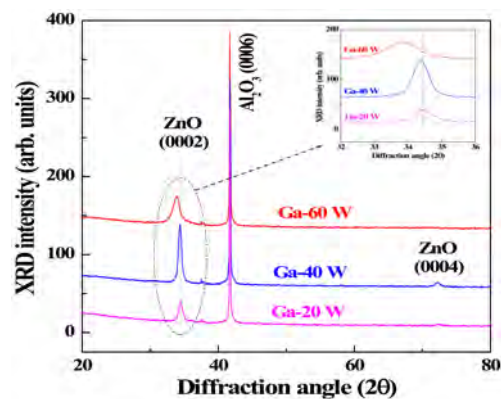


Fig. 1. Rocking curves of the XRD ω - 2θ scans on the RT grown ZnO : Ga layers by varying the RF power of Ga_2O_3 target. Also, a portion of the XRD ω - 2θ scans was magnified in the subfigure.

Table 1. The structural parameters of ZnO : Ga obtained from the XRD experiment by varying the RF power of the Ga_2O_3 target.

| Ga content by RF-power variation | Lattice constant (nm) | Biaxial stress (GPa) | FWHM (degree) | Mean crystallite size (nm) |
|----------------------------------|-----------------------|----------------------|---------------|----------------------------|
| Ga-20 | 0.5207 | -0.0871 | 0.3135 | 28 |
| Ga-40 | 0.5212 | -0.5228 | 0.2695 | 33 |
| Ga-60 | 0.5286 | -6.9704 | 0.5160 | 16 |

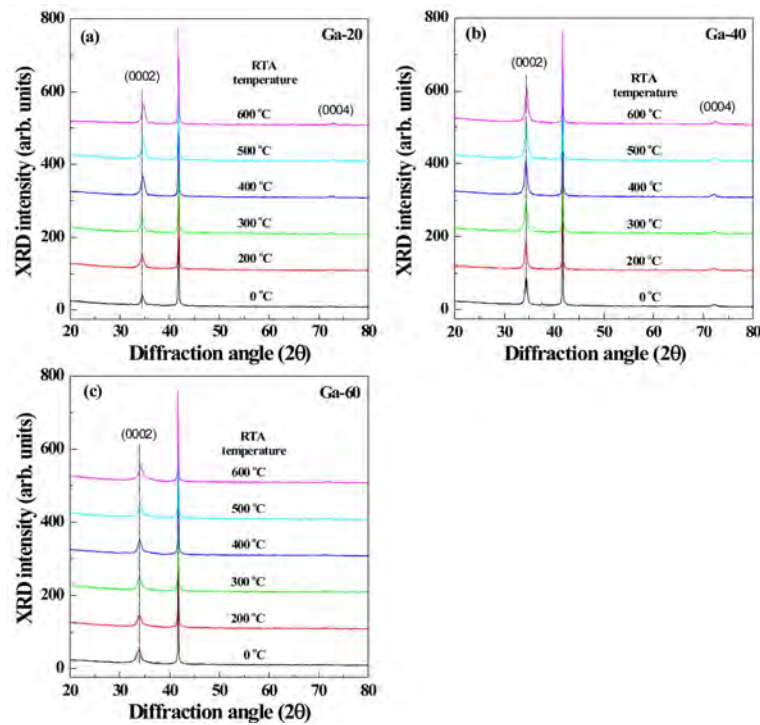


Fig. 2. Rocking curves of the XRD ω - 2θ scans with and without RTA process on the RT grown ZnO : Ga layers.

be enhanced with the increase of the Ga contents as shown in Table 1. Therefore, the lattice parameter of the c-axis is increased with the increase of the RF power of Ga₂O₃ target.

On the other hand, Ga-40 of the ZnO : Ga layers showed an excellent crystallinity. The XRD spectrum of Ga-40 had a strong intensity and small FWHM value. Thus, it is estimated that the lattice parameter on the c-axis of Ga-40 corresponds to the composition rate, having the Ga₂O₃ amount of the 3-wt.% added to the ZnO powder target as a dopant [12].

Characteristic property of rapid-thermal post-annealing on RT as-grown ZnO : Ga layers

In order to improve the crystal quality of the RT as-grown ZnO : Ga layers, the ZnO : Ga layers were post-annealed by using the RTA method with the temperature variation from 200 to 600 °C for 1 min in a N₂ atmosphere. Fig. 2 shows the rocking curves of the XRD ω - 2θ scans with and without RTA process on the RT grown ZnO : Ga layers. As shown in Fig. 2, the peak intensity on (0002) phase of Ga-20 and Ga-40 showed a tendency of the increase by increasing the RTA temperature and its intensity saturated at RTA temperatures over 400 °C. Furthermore, the new (0004) plane from Ga-20 appeared at RTA temperatures over 400 °C. It suggests that the crystalline of the layers, due to the post annealing, has strongly improved the c-axis of hexagonal structure according to the increase of RTA temperature. But the peak intensity on Ga-60 hardly changed in spite of increasing the RTA temperature. The peak positions of the post-annealed

(0002) plane at high temperatures over 500 °C in Ga-20 and Ga-60 are slightly shifted to high diffraction angle. As compared with the layers without the RTA process, these ZnO : Ga layers have a larger diffraction angle and small lattice constants. This result concludes that the role of Ga atoms by the high RTA temperature changed the interstitial atoms into the substitutive atoms in the ZnO lattices. Most parts of the Ga substitutes for Zn make the c-axis shorter, because the ionic radius of Ga is smaller than that of Zn.

Fig. 3 shows the transmittance with and without the RTA process on the RT grown ZnO : Ga layers. As shown in Fig. 3, the curves of the RTA process at low temperatures below 300 °C showed a tendency of the low transmittance below 70%. For the Ga-40 case, the transmittance curves at RTA temperatures over 300 °C were very transparent with transmittance exceeding 80% indicating good optical quality in the whole visible range. Thus, the curves of the steep gradient clearly indicate the relaxation of the compressive strain remaining in Ga-40. Also, at the RTA temperature of 500 °C, the transmittance is nearly over 95%, while the transparent degree at RTA temperature of 600 °C was reduced. Therefore, it indicates that RTA temperatures over 600 °C are too high, deteriorating the crystal quality of the ZnO : Ga layers. In order to extract the band-gap energy from the transmittance result, the model for direct inter-band transitions is generally used as $(\alpha h\nu)^2 = A(h\nu - E_g)$. Here, A is a function of the refractive index and the hole/electron effective masses, and $h\nu$ is the energy of the incident photon. Also, α and E_g are the absorption coefficients and the band-gap

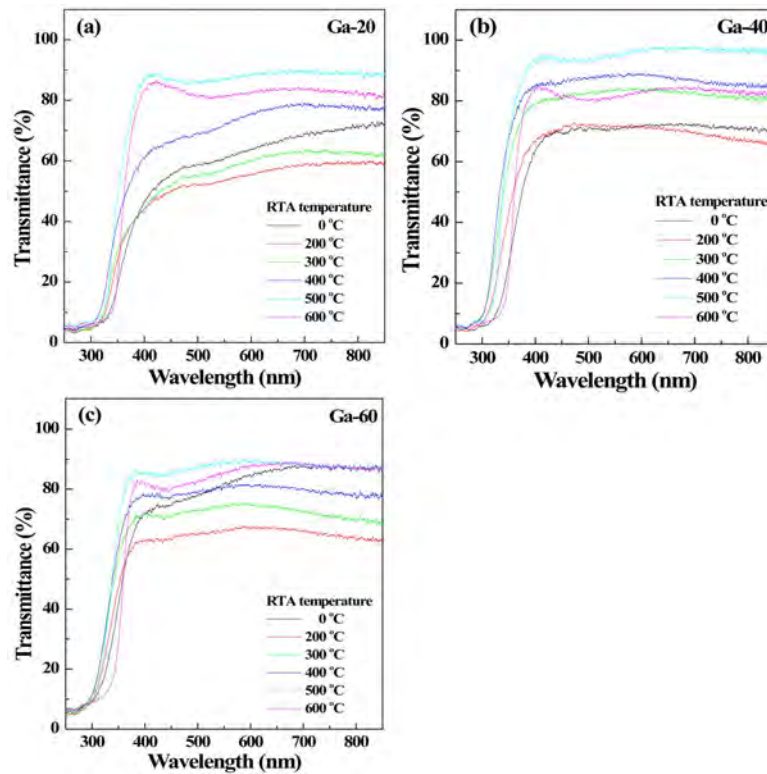


Fig. 3. Transmittance with and without the RTA process on the RT grown ZnO : Ga layers.

energy, respectively. Fig. 4 displays a plot of $(\alpha h\nu)^2$ as a function of photon energy according to the RTA-temperature variation of Ga-40. The E_g can be evaluated from the interception of the extrapolated linear part of the curve with the energy axis. Also, the subfigure shows the values of E_g as a function of RTA temperature. As shown in the subfigure, the optical band-gap energy ranges from 3.4548 to 3.8118 eV according to the variation of the RTA temperature. At this time, the E_g increased during the increase of the RTA temperature. Thus, it showed the maximum value at the RTA temperature of 400 °C and then a decrease was observed. This situation can be explained from the temperature of the RTA process on the ZnO : Ga layers. It relates to the fact that the Ga atoms have been incorporated into the layer due to the RTA process. If the Ga atoms are located at substitution sites, then there is an increase in the carrier concentration. Consequently, the variation of E_g with annealing temperature of RTA could attribute to band gap widening due to the Burstein-Moss (BM) effect and band gap narrowing due to many body effects [13]. In the model of BM, the absorption edge shift in an n -type semiconductor is dependent on carrier concentration [14, 15]. Also, the electronic states in heavily doped and highly excited semiconductors are modified because of carrier-carrier interaction and carrier-impurity interactions. Therefore, many body effects of these interactions lead to a narrowing of the band gap [16].

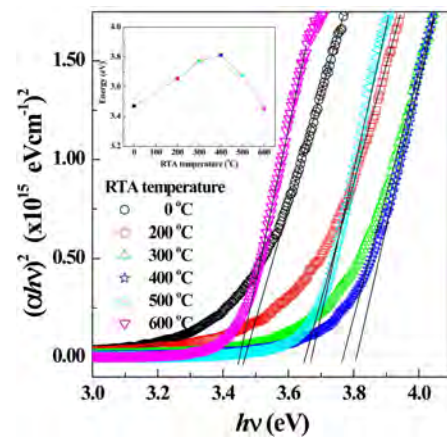


Fig. 4. Plot of $(\alpha h\nu)^2$ as a function of photon energy according to the RTA-temperature variation of Ga-40. The subfigure shows the values of E_g as a function of RTA temperature.

Fig. 5 presents resistivity and sheet resistance according to the variation of the RTA temperature. The resistivity and sheet resistance decreased when increasing the RTA temperature from 0 to 400 °C, and then they again increased to the RTA temperature of 600 °C. At low RTA temperatures, it suggests that high resistivity of the ZnO : Ga layers results in degraded crystallinity and few Ga substitutions. While large resistivity at high RTA temperatures of over 500 °C relates to carrier-impurity interactions, this acts as the cause, deteriorating the crystal quality of the ZnO : Ga layers, due to the increase in the carrier concentration.

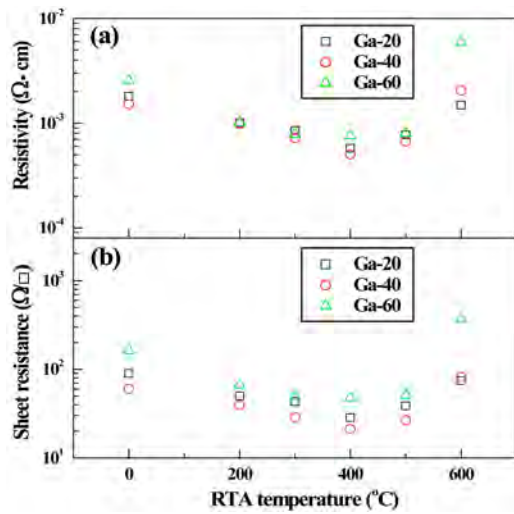


Fig. 5. Resistivity and sheet resistance according to the variation of the RTA temperature.

At this time, the lowest value of resistivity and sheet resistance was observed from Ga-40, annealed at 400°C ; their values were $5.04 \times 10^{-4} \Omega \cdot \text{cm}$ and $21.24 \Omega/\square$, respectively. Thus, it suggests that the optimum RTA process of 400°C can improve the layer crystallinity and Ga substitution in ZnO. This value is nearly equal to the value of $4.54 \times 10^{-4} \Omega \cdot \text{cm}$ of the ZnO:Ga layer grown on the Si substrate by MOCVD [17]. However, our resistivity value is lower than that of $7.2 \times 10^{-3} \Omega \cdot \text{cm}$ on the Ga-doped ZnO layer grown on the Al_2O_3 substrate by MOCVD [18].

ZnO:Ga layers grown with varying substrate temperature

In order to grow ZnO:Ga layers through the substrate-temperature variation, the RF power of the ZnO and Ga_2O_3 targets was fixed to 80 and 40 W, respectively, and the substrate temperature was varied to the intervals of 200°C from RT (0) to 600°C . Fig. 6 presents the rocking curves of the XRD ω - 2θ scans on the ZnO:Ga layers grown with the variation of the substrate temperature. As shown in Fig. 6, two dominant peaks, except the substrate peak of Al_2O_3 (0006), appeared in each spectrum. These patterns associated with the diffraction peaks corresponding to the (0002) and (0004) phase of ZnO. When increasing substrate temperature, these spectra had a strong intensity and a narrow FWHM value. As the subfigure in Fig. 6 shows, the layer peak grown at 400°C is nearly ZnO (0002) phase, which indicates the formation of stoichiometric ZnO layers.

Fig. 7 displays the transmittance spectra on the ZnO:Ga layers grown with the variation of the substrate temperature. The ZnO:Ga layer grown at RT is poor in quality for transmittance and crystallinity. However, the ZnO:Ga layer grown at 400°C shows the abrupt curvature and the average transmittance of

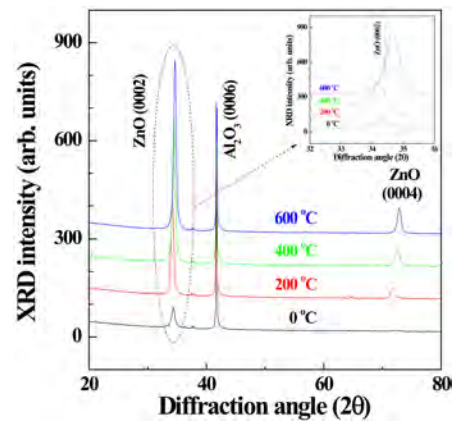


Fig. 6. Rocking curves of the XRD ω - 2θ scans on the ZnO:Ga layers grown with the variation of the substrate temperature.

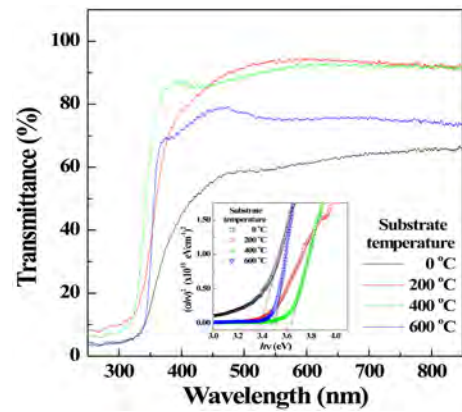


Fig. 7. Transmittance spectra on the ZnO:Ga layers grown with the variation of the substrate temperature.

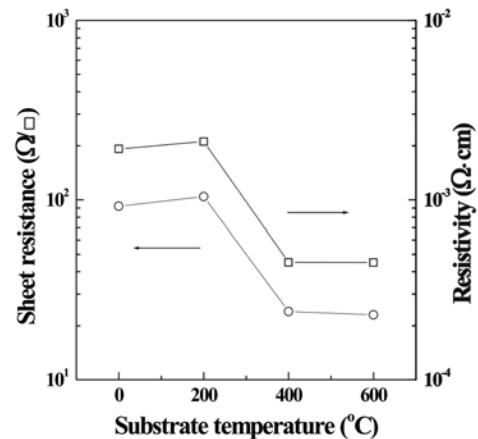


Fig. 8. Sheet resistance and resistivity as a function of the substrate-temperature variation.

over 90% in the visible-wavelength region. This suggests that high transmittance due to the reduction of scattering and absorption leads to high crystal quality. The subfigure in Fig. 7 shows the plot of $(\alpha h\nu)^2$ as a function of photon energy on the ZnO:Ga layers. The optical band gap energies on the temperature variation of the substrate were posited from 3.3930 to 3.6427 eV. As shown in the subfigure, optical band gap energy of

the ZnO : Ga layer grown at 400 °C was larger than other layers. It indicates that the ZnO : Ga layer grown at 400 °C has a good crystalline quality.

Fig. 8 presents the sheet resistance and resistivity as a function of the substrate-temperature variation. The sheet resistance and resistivity at a low substrate temperature had high values, while those with the substrate temperature of 400 and 600 °C showed low values. At this time, the sheet resistance and resistivity were about 23 Ω/\square and $4.5 \times 10^{-4} \Omega \cdot \text{cm}$, respectively. These values are nearly equal to those of the layer post-annealed at 400 °C after the RT growth. By comparing the ZnO : Ga layers processed by RTA after the RT growth and grown with varying substrate temperatures, a useful result could be extracted. The growth of ZnO : Ga layers by heating the substrate requires any high growth temperature. In some cases, they need to continue the post annealing process for a long time. Thus, these processes disturb the concise fabrication of ZnO : Ga. Consequently, these results indicate that the optimum RTA process after RT growth can shorten and simplify the complicated fabrication of the ZnO : Ga layers.

Conclusions

The ZnO : Ga layers were grown on the Al_2O_3 substrate by using the RF magnetron co-sputtering system at RT plus varying the RF power of the Ga_2O_3 target. The grown ZnO : Ga layers were post-annealed by the RTA method using various temperatures. Ga-40 of the RT as-grown ZnO : Ga layers showed an excellent crystallinity. Thus, its lattice parameter corresponds to the composition rate having the Ga_2O_3 amount of the 3-wt.% added to the ZnO powder target as a dopant. After the RTA process, the crystalline of the layers was observed to be improved on the c-axis of hexagonal structure according to the increase of the RTA temperature. From the transmittance, the transmittance curves on Ga-40 of the RTA temperatures over 300 °C were very transparent, with transmittance exceeding 80%, indicating good optical quality in the whole visible range and it showed the curves of the steep gradient, meaning the relaxation of the compressive strain, remaining in layer. Also, the optical band-gap energy ranged from 3.4548 to 3.8118 eV according to the variation of the RTA temperature. This band-gap energy showed a tendency to increase until the RTA temperature of 400 °C and then a decrease was observed. It was interpreted that the variation of E_g according to the annealing temperature of RTA was attributed to band gap widening due to the BM effect and band gap narrowing due to many body effects. From the resistivity and sheet resistance, the lowest values were observed from Ga-40 annealed at 400 °C; their values were $5.04 \times 10^{-4} \Omega \cdot \text{cm}$ and $21.24 \Omega/\square$,

respectively. On the other hand, a bunch of the ZnO : Ga layers were grown with the substrate-temperature variation. The ZnO : Ga layers grown at the substrate temperature of 400 °C had a good crystalline quality. Their results were nearly equal to those obtained from the layer that was post-annealed at 400 °C after the RT growth. Consequently, we suggest that the RTA process after the RT growth can shorten and simplify the complicated fabrication of the ZnO : Ga layers for device applications.

Acknowledgments

This research was supported by Basic Science Research Program through the National Research Foundation of Korea (NRF) funded by the Ministry of Education (2009-0094031).

References

1. C. Kittel, "Introduction to solid state physics" 5th ed. Wiley. (1976) 100.
2. Q.B. Ma, Z.Z. Ye, H.P. He, S.H. Hu, J.R. Wang, L.P. Zhu, Y.Z. Zhang and B.H. Zhao, *J. Cryst. Growth.* 304 (2007) 64-68.
3. D.H. Oh, Y.S. No, S.Y. Kim, W. J. Cho, J.Y. Kim and T.W. Kim, *J. Ceram. Process. Res.* 12 (2011) 488-491.
4. G.A. Hirata, J. McKittrick, T. Cheeks, J.M. Siqueiros, J.A. Diaz, O. Contreras and O.A. Lopez, *Thin Solid Films.* 288 (1996) 29-31.
5. A. Behrends, A. Wagner, M.A.M. Al-Suleiman, H. Lugauer, M. Strassburg, R. Walter, A. Weimar, A. Waag and A. Bakin, *Phys. Status Solidi A* 209 (2012) 708-713.
6. K.T.R. Reddy, T.B.S. Reddy, I. Forbes and R.W. Miles, *Surf. Coat. Tech.* 151-152 (2002) 110-113.
7. J.H. Kim, B.D. Ahn, C.H. Kim, K.A. Jeon, H.S. Kang and S.Y. Lee, *Thin Solid Films.* 516 (2008) 1330-1333.
8. G.J. Fang, D. Li and B.L. Yao, *Thin Solid Films.* 418 (2002) 156-162.
9. X.Yu, J. Ma, F. Ji, Y. Wang, X. Zhang and H. Ma, *Thin Solid Films.* 483 (2005) 296-300.
10. B.D. Cullity, *Elements of X-Ray Diffractions*, (Addition-Wesley, 1978) p. 102.
11. C.V. Ramana, R. J. Smith, O.M. Hussain and C.M. Julien, *Mater. Sci. Eng B* 111 (2004) 218-225.
12. L. Fang, K. Zhou, F. Wu, Q.L. Huang, X.F. Yang and C.Y. Kong, *J. Supercon. Nov. Magn.* 23 (2010) 885-888.
13. J.G. Lu, S. Fujita, T. Kawaharamura, H. Nishinaka, Y. Kamada, T. Ohshima, Z.Z. Ye, Y.J. Zeng, Y.Z. Zhang, L.P. Zhu, H.P. He and B.H. Zhao, *J. Appl. Phys.* 101 (2007) 083705-1-083705-7.
14. E. Burstein, *Phys. Rev.* 93 (1954) 632-633.
15. T.S. Moss, *Proc. Phys. Soc. Sect B* 67 (1954) 775-782.
16. D. Auvergne, J. Camassel and H. Mathieu, *Phys. Rev B* 11 (1975) 2251-2259.
17. Y.C. Huang, Z.Y. Li, L.W. Weng, W.Y. Uen, S.M. Lan, S. M. Liao, T.Y. Lin, Y.H. Huang, J.W. Chen, T.N. Yang, C. C. Chiang, *Vac. Sci. techol A* 27 (2009) 1260-1265.
18. A. Behrends, A. Wagner, M.A.M. Al-Suleiman, H.J. Lugauer, M. Strassburg, R. Walter, A. Weimar, A. Waag and A. Bakin, *Phys. Status Solidi A* 209 (2012) 708-713.